PROCEEDINGS OF SCIENCE

Background study for Korea Experiments on Magnetic Monopole

Changgi Huh,[a,*] **John Hauptman,**[c] **Sehwook Lee,**[a] **Min Sang Ryu,**[b] **Junghyun Lee,**[a] **Bobae Kim,**[a] **Yun Eo**[d] **and Hwidong Yoo**[d]

[a] *Department of Physics, Kyungpook National University, Daegu 41566, Korea*
[b] *The Center for High Energy Physics, Kyungpook National University, Daegu 41566, Korea*
[c] *Department of Physics and Astronomy, Iowa State University, Ames 50011, USA*
[d] *Department of Physics, Yonsei University, Seoul, 03722, Korea*

E-mail: changgi.huh@cern.ch, hauptman@iastate.edu, seh.wook.lee@cern.ch

Elementary magnetic monopoles have been a question of electromagnetism for the last 150 years. However, most monopoles have been searched in the large mass and large magnetic charge region during the period but have not been discovered yet. Therefore, assuming that monopoles may exist in the low mass and low charge regions, we designed an experiment to search for elementary magnetic charges with mass below the electron mass (m_e) and charge below the electron charge (e). In this talk, we will describe the design for the experiment, and present the prediction of event rates, energy resolutions of detectors, and potential backgrounds estimated with GEANT4 simulations.

41st International Conference on High Energy physics - ICHEP2022
6-13 July, 2022
Bologna, Italy

*Speaker

PoS(ICHEP2022)1026

1. Introduction

We search for magnetic charged (g) particles with mass less than the electron mass. The e^+e^- annihilates at rest through a virtual photon. That virtual photon couples to a magnetic charge-anti charge pair m^+m^- with a coupling proportional to g^2,

$$\alpha_{m^+m^-} = \frac{g^2}{4\pi\epsilon_0\hbar c},$$

which is illustrated in Figure 1.

^{22}Na is a positron source that can be embedded in the annihilation target and which yields a low energy positron (e^+) at $E_{e^+} < 0.545$ MeV that precedes by 3.7 ps a photon (γ) at $E_\gamma = 1.275$ MeV. The positron annihilates on an atomic electron near rest in a metallic target within a few picoseconds [1] yielding two back-to-back 0.511-MeV γs. The 1.275-MeV γ is used as a pre-trigger or start-of-event signal.

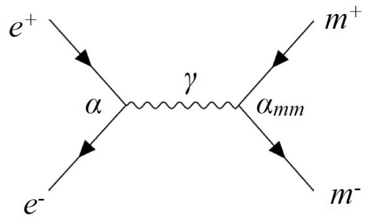

Figure 1: Feynman diagram for $e^+e^- \to \gamma^* \to m^+m^-$.

For a magnetic charge, g, in our uniform solenoidal field of $\int B_z dz \approx 1$T·m the energy gain is

$$\Delta E = (300 \text{ MeV}) \times g/e.$$

Therefore, we are sensitive down to $g/e \approx 10^{-2}$ where the total magnetic particle energy is ~ 6 MeV compared to the ^{22}Na positron source energies of 1.27 and 0.511 MeV.

2. Simulation Setup

The simulation was performed with the GEANT4 (release 10.4.0) FTFP-BERT physics list to estimate the physical background.
^{22}Na positron source and the 10 μm aluminum target are located in the center of the chamber, and a trigger-veto detector surrounds them. A 1T solenoid surrounds 1 m of the vacuum cylinder, and end-cap calorimeters are located on both ends as shown in Figure 2.

We calibrate the particle's energy from the number of measured photoelectrons in the SiPM. The 662 keV gamma rays are used to calibrate detectors. We use a trigger-veto detector and end-cap calorimeter using 662 keV and 1 MeV gamma rays to validate the calibration coefficient. The single crystal calibration constant is well performed in full detectors.

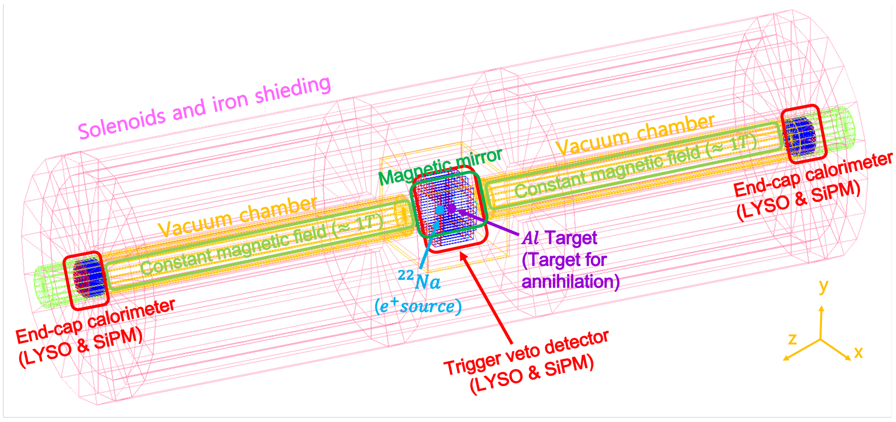

Figure 2: Geometrical aspects of the simulations.

3. Results

Backgrounds to a signal of a magnetic charge-anti charge pair can be separated into (*i*) ^{22}Na positron source related, (*ii*) intrinsic radioactivity from LYSO associated, (*iii*) cosmic muons, both correlated and uncorrelated, (*iv*) cosmic electromagnetic particles, both correlated and uncorrelated. Those results are shown in Figure 3.

Pattern recognition consists of clustering repeated Compton scatters in the crystal array. The pattern recognition, D_{xy}, is

$$D_{xy} = \sqrt{\frac{\sum d_i^2 E_i}{\sum E_i}}$$

where $d_i = \sqrt{(x_i - x_0)^2 + (y_i - y_0)^2}$ is distance between crystal and hit position, x_i, y_i, and E_i is position and energy of trigger-veto detector and end-cap calorimeter. $x_0 = \sum x_i E_i / \sum E_i$, $y_0 = \sum y_i E_i / \sum E_i$, is the position calculated from the center-of-energy method using the nearest crystals from the hottest crystal in the trigger-veto detector and end-cap calorimeter. Figure 4 shows D_{xy} distributions of the trigger-veto detector and end-cap calorimeter with 1 or 2 γs with receiver operating characteristic curve in the trigger-veto detector and end-cap calorimeter.

The four different types of physical backgrounds are considered. From the ^{22}Na simulation, we can precisely measure the trigger signal in the trigger-veto detector. It does not leave energy in the magnetic monopole search region. From the pattern recognition, the efficiencies of single and multiple particle discrimination from the trigger-veto detector and end-cap calorimeter are 90% and 95%, respectively, at 95% background rejection. The intrinsic radioactivity does not affect both the trigger signal and the monopole search region. The cosmic muons and electromagnetic particles leave energy up to 1 GeV in calorimeters. Those directly affect the monopole search region. However, we can veto these with a coincidence of another muon veto detector surrounding the trigger-veto detector and end-cap calorimeters.

References

[1] C. Hugenschmidt, “Positrons in Surface Physics,” arXiv:1611.04430v1, 14 Nov 2016.

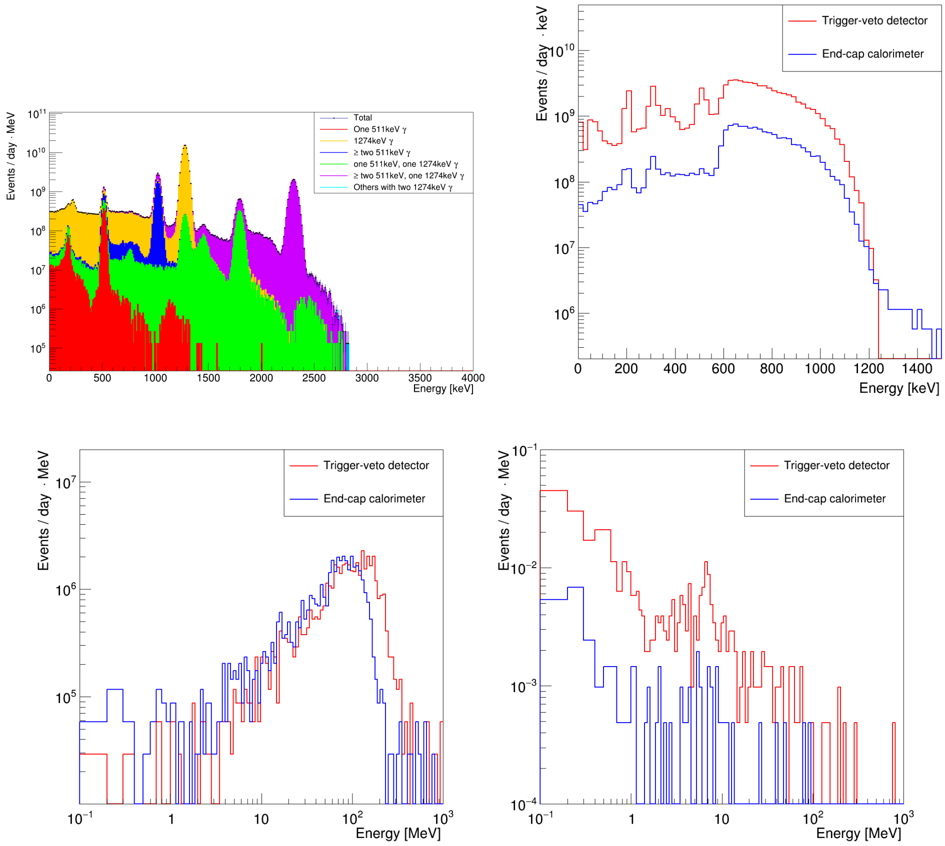

Figure 3: ^{22}Na positron source related (top left), intrinsic radioactivity from LYSO related (top right), cosmic muons, both correlated and uncorrelated (bottom left), cosmic electromagnetic particles, both correlated and uncorrelated (bottom right)

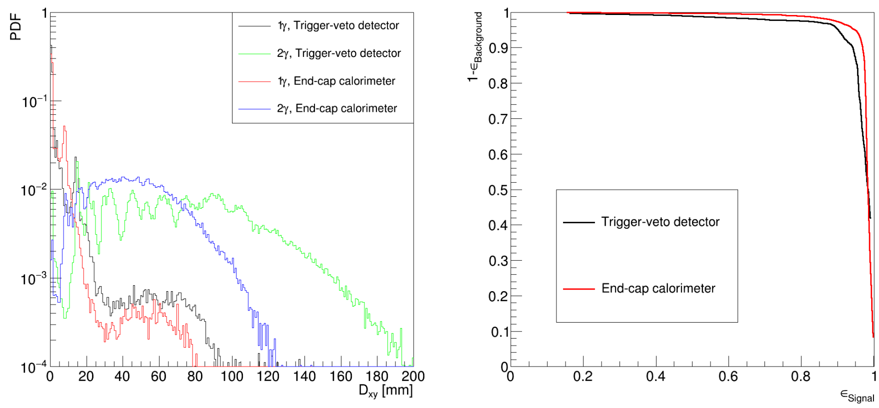

Figure 4: Pattern recognition distribution in the trigger-veto detector and end-cap calorimeter. (left) Receiver operating characteristic curve in the trigger-veto detector and end-cap calorimeter. (right)